



AUTHOR(S):

TITLE:

YEAR:

Publisher citation:

OpenAIR citation:

Publisher copyright statement:

This is the _____ version of proceedings originally published by _____
and presented at _____
(ISBN _____; eISBN _____; ISSN _____).

OpenAIR takedown statement:

Section 6 of the “Repository policy for OpenAIR @ RGU” (available from <http://www.rgu.ac.uk/staff-and-current-students/library/library-policies/repository-policies>) provides guidance on the criteria under which RGU will consider withdrawing material from OpenAIR. If you believe that this item is subject to any of these criteria, or for any other reason should not be held on OpenAIR, then please contact openair-help@rgu.ac.uk with the details of the item and the nature of your complaint.

This publication is distributed under a CC _____ license.

Comparison of artificial neural network and multiple regression for partial discharge sources recognition

Abdullahi Abubakar Mas'ud^{1,*}, Firdaus Muhammad-Sukki², Ricardo Albarracín³, Jorge Alfredo Ardila-Rey⁴, Siti Hawa Abu-Bakar⁵, Nur Fadilah Ab Aziz⁶, Nurul Aini Bani⁷, Mohd Nabil Muhtazaruddin⁷

¹ Department of Electrical and Electronic Engineering Technology, Jubail Industrial College, P O Box 10099, Saudi Arabia

² School of Engineering, Robert Gordon University, Garthdee Road, Aberdeen AB10 7GJ United Kingdom

³ Department of Electrical, Electronic and Automation Engineering and Applied Physics, Senior Technical School of Engineering and Industrial Design (ETSIDI), Polytechnic University of Madrid (UPM), Ronda de Valencia 3, Madrid 28012, Spain

⁴ Department of Electrical Engineering, Universidad Técnica Federico Santa María, Santiago de Chile 8940000, Chile

⁵ Universiti Kuala Lumpur British Malaysian Institute, Batu 8, Jalan Sungai Pusu, 53100 Gombak, Selangor, Malaysia

⁶ Department of Electrical Power Engineering, College of Engineering, Universiti Tenaga Nasional, KM-7, Jalan Kajang-Puchong, 43009 Kajang, Selangor, Malaysia

⁷ UTM Razak School of Engineering and Advanced Technology, Universiti Teknologi Malaysia Kuala Lumpur, Jalan Sultan Yahya Putra 54100 Kuala Lumpur, Malaysia

* Email addresses: masud_a@jic.edu.sa

Abstract- This paper compares the capabilities of the artificial neural network (ANN) and multiple linear regression (MLR) for recognizing and discriminating partial discharge (PD) defects. Statistical fingerprints obtained from a several PD measurement were applied for training and testing both the ANN and MLR. The result indicates that for both the ANN and MLR trained and tested with the same insulation defect, the ANN has better recognition capability. But, when both ANN and MLR were trained and tested with different PD defects, the MLR is generally more sensitive in discriminating them. In this paper, the results were evaluated for practical PD recognition and it shows that both of them can be used simultaneously for both online and offline PD detection.

Keywords - Partial discharge; regression analysis; artificial neural network.

I. INTRODUCTION

Partial discharge (PD) is a breakdown activity commonly found in the high-voltage (HV) insulation apparatus [1]. It often leads to changes in electrical field configuration accompanied by sustained electrical discharges. If PD, such as internal, is not detected at the initial stage, these discharges can bridge the insulation system with complete breakdown of the insulation and serious financial implications [2]. Therefore, PD measurement and recognition has been the focus of condition monitoring engineers [3].

Over the years, much effort has been exhausted in applying the artificial neural network (ANN) in recognizing a number of PD defects and tremendous success has been recorded [1, 4].

This is because the ANN has the capability to learn from few training data. However, ANN has number of disadvantages, which include lengthy training time and sensitivity to different initial weights and biases [4]. Of recent multiple linear regression (MLR) has shown the potential for accurate PD recognition [5]. However, it has not applied to recognize and discriminate complex PD patterns. Therefore this paper compares the capabilities ANN and MLR to recognize and discriminate PD patterns in order to understand to identify a robust system for both online and offline PD detection. Both the ANN and MLR will be trained and tested using statistical features of the PD patterns. These statistical fingerprints are extracted from the φ - q - n (phase-amplitude-number) patterns representing different PD sources. For φ - q - n evaluation, statistical fingerprints have been widely applied because of their capability for well-defined pattern quantification [1, 3]. In order to simplify the φ - q - n analysis, statistical fingerprints are usually extracted from 2D plots derived from the φ - q - n patterns. The main 2D distributions of interest are the pulse count $H_n(\varphi)$, mean pulse-height $H_{qn}(\varphi)$ and amplitude number $H_n(q)$ plots. These plots are presented in both the positive (+) and negative half power cycles (-) [4].

The overall aim of this paper is to classify and discriminate different PD patterns commonly occurring in practice using the ANN and MLR and to compare the result in order to determine the robust for practical application. PD data captured over long stressing period will be applied for training and testing both the ANN and MLR models.

II. PD MEASUREMENT SET UP

The PD measurement process was carried out in accordance with the IEC 60270 PD Standard 2001 [6]. The PD detection system developed in the HV laboratory of Glasgow Caledonian University produces real time ϕ - q - n patterns and possesses functions for automatic data logging patterns at different time periods as well as controlling changes in the resolution sizes. This is vital for the work presented in this paper, as several experiments require longer stressing period and data and must be captured and stored systematically over fixed resolution size for a more reliable analysis. PD calibration was carried out for PD apparent charge determination. In this paper, four PD sources were manufactured. These include corona in air, corona in oil, internal PD in a single void from polyethylene-terephthalate (PET) PET and surface PD in air, as illustrated in Fig. 1.

The corona discharge model is a point-plane configuration as shown in Fig. 1(a). A needle of length 3cm and tip radius 10mm is connected to the HV, while an electrode of 60mm in diameter is connected to the ground. Two points to ground gap distances are considered namely 5mm and 10mm. Test voltages are 1.5kV 1.9kV 2kV and 2.2kV for the 5mm gap and 1.7kV 1.9kV 2.3kV and 2.8kV for the 10mm gap distance. Measurements were taken at different voltages over 2 gap distances of 5mm and 10mm because of the PD behavior of the positive corona discharge. They have low repetition rate and higher amplitude [7]. They are then combined to form ϕ - q - n corona set for evaluation by the ANN and MLR models.

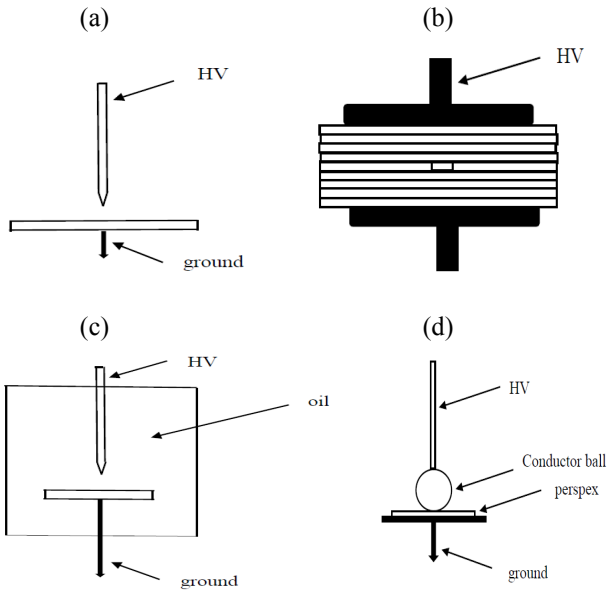


Fig 1: Manufactured PD faults: (a) corona PD in air; (b) internal PD into a void in PET; (c) corona PD in oil, and d) surface discharge in air.

Corona PD in oil is studied from a point-plane configuration immersed in Castrol insulating oil (see Fig. 1(c)). The applied voltage was 28kV and a needle electrode was placed at a distance of 25mm from a ground plane. In all the experiments, only a few discharges were seen to occur within both half-power cycles and these observations are consistent with other previously published work literature [8].

For the single void experiments, measurements were made with 5mm void created at the center of the PET layers, Fig. 1(b). Nine layers were created similar to the literature [3]. The inception voltage for void 5 was 3.4kV and all measurements were taken at approximately 4.4kV. PD data was captured over 250 power cycles from the start up to 7-hours continuous stressing.

Surface PDs in air were studied by placing a small brass ball of 55mm diameter on Perspex insulation as shown in Fig. 1d. The Perspex is of size 65mm x 65mm x 8mm. The inception voltage is 4.2kV and the experiment was carried out at 20% above the PD inception voltage. The Perspex was stressed up to 4hours and ϕ - q - n patterns recorded for up to 4hours.

III. THE NEURAL NETWORK

ANNs are mathematical models that imitate the way humans, learn tasks, classify patterns and find solutions to problems [9, 10]. The multilayer perceptron neural network (MLPN) using the back propagation (BP) is the most widely applied for PD classification because of its capability to classify complex PD fingerprints [1, 3]. The basic structure of an MLPN consists of the input layer, hidden layer and the output layer. However, it can have many layers and normally has sigmoid-type functions in the hidden layer. There are no certain criteria for selecting the number of neurons in the hidden layer, but enough neurons are needed to obtain a very good performance. The MLPN is a feed forward network (Fig. 2) where the training parameters move from the input layer to the hidden layer and finally to the output layer. The MLPN is trained in such a way as to find the weight that minimizes the mean square error (MSE) at the output, i.e. when the output closely matches the target output.

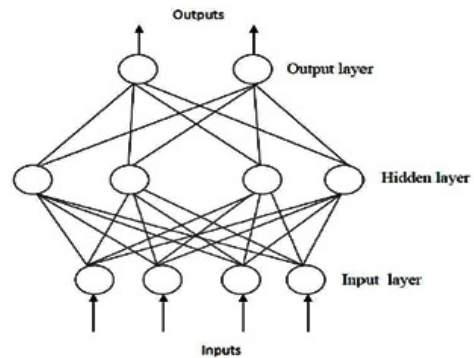


Fig 2: The MLPN.

In designing and training the MLPN, certain considerations have to be taken to be able to get the best performance, i.e. by choosing the number and types of neurons in the hidden layer and finding the best solution to avoid local minima in the error space. Local minima are a sudden termination of the training error curve resulting from instability of the ANN [9]. In this paper, the MLPN will be applied to classify different PD fault geometries and the results were compared with that of the MLR model.

IV. MULTIPLE LINEAR REGRESSION

The MLR adopts a linear relationship between a dependent variable y_j and a set of descriptive variables or regressors $x'_j = (x_{j0}, x_{j1}, \dots, x_{jN})$. The first regressor $x_{j0} = 1$ is a constant [5, 11]. For a sample having M observations, every observation j can be expressed according to an equation forms as [11]:

$$y_i = x'_j \beta + \alpha_j \quad (1)$$

where β is a $(N + 1)$ column parameter vector, x'_j is a $(N+1)$ row vector and μ represent an error vector. Equation (1) can be compactly written as:

$$y_i = X\beta + \alpha \quad (2)$$

where y is a M- column dimensional vector, X is a $M \times (N + 1)$ matrix and α is a M-column dimensional vector consisting of error terms.

To predict the value of β , least squares approach similar to simple linear regression case is adopted, i.e. to minimize over all possible intercepts.

$$\sum_j (y_j - \beta_1 X_{j,1} \dots \beta_{N+1} X_{j,N+1}) \quad (3)$$

Equation (3) is actually minimized by setting:

$$\hat{\beta} = (X'X)^{-1} X'Y \quad (4)$$

V. PD FINGERPRINTS FOR ANN AND MLR

For φ - q - n analysis, statistical fingerprints were widely applied because of their capability for well-defined pattern quantification [1, 3, 12]. In order to simplify the φ - q - n evaluation, statistical fingerprints are usually extracted from 2D plots derived from the φ - q - n patterns. The key 2D distributions of interest are the pulse count $H_n(\varphi)$, mean pulse-height $H_{qn}(\varphi)$ and amplitude number $H_n(q)$ plots. These plots are presented in both the positive (+) and negative half power cycles (-). This

paper applies 15 statistical parameters that serve as input fingerprints for training and testing both the ANN and MLR. These include the skewness (sk) and Kurtosis (ku) of the $H_{qn}(\varphi)+$, $H_{qn}(\varphi)-$, $H_n(q)+$, $H_n(q)-$, $H_n(\varphi)+$ and $H_n(\varphi)-$ distributions, the cross-correlation (cc), discharge factor (Q) and modified cross-correlation (mcc). Out of this statistical fingerprints, the sk and ku of the $H_n(q)$ have never being applied for complex PD evaluation and will therefore be applied in this paper.

The sk and ku are determined as follows:

$$sk = \frac{\sum (x_j - \mu)^3 P_j}{\sigma^3} \quad (5)$$

$$ku = \frac{\sum (x_j - \mu)^4 P_j}{\sigma^4} \quad (6)$$

where μ is the average value, σ is the standard deviation and P_j is the probability of the discrete value x_j and y_j as the case may be.

The Q and cc are determined as follows:

$$Q = \frac{Q_S^- / N_S^-}{Q_S^+ / N_S^+} \quad (7)$$

$$cc = \frac{\sum x_j y_j - \frac{\sum x_j \sum y_j}{n}}{\sqrt{\left[\sum x_j^2 - \frac{(\sum x_j)^2}{n} \right] \left[\sum y_j^2 - \frac{(\sum y_j)^2}{n} \right]}} \quad (8)$$

where mcc is the product of Q and cc . n represent the sample size of the data. Q_S^+ and Q_S^- represent the sum of discharge amplitudes in both the +ve and negative half power cycles, Similarly N_S^+ and N_S^- represent the number of discharges in both the +ve and -ve half power cycle.

Figs. 3-6 compare the 95% limits for several statistical parameters when applied as input to the ANN and MLR. Four statistical parameters (Q , cc , sk ($H_n(\varphi)+$), ku ($H_{qn}(\varphi)+$)) were chosen for comparison because they show clear discrimination between the PD patterns as compared to the other fingerprints. From Fig. 3, it is obvious that corona in air has the least value of Q . This is expected, as there are few PD pulses in the positive half cycle of cycle of corona. The average value of Q for corona in oil and void are almost close to 1 showing similarity in their discharge amplitude distribution in both half of the power cycles. It is also evident that the cc for corona type discharges is low compared to void and surface discharges showing highly asymmetrical positive and negative half cycle discharges (Fig. 4). From Fig. 5, it can be seen that the sk of $H_n(q)+$ have wider

complete intervals for corona in air and void as compared to the others because of large number of discharges with lower amplitude level with uneven distribution. The ku of the $H_{qn}(\varphi)+$ distributions appears to be more peaked for corona in air and surface discharges as compared to the others. This shows that the mean discharges are concentrating within certain amplitude levels unlike the others that have wider distribution of discharges over the φ - q - n plane.

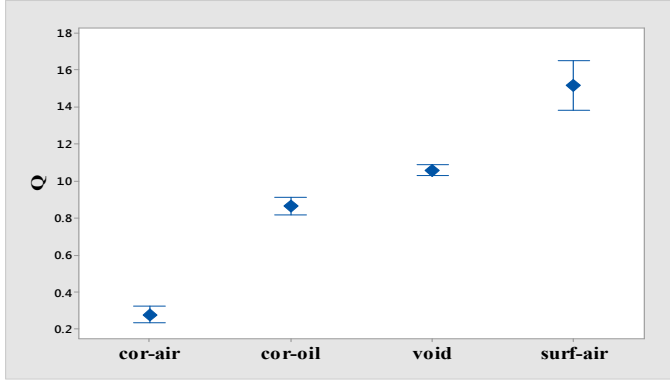


Fig. 3: Comparison of Q for different PD sources.

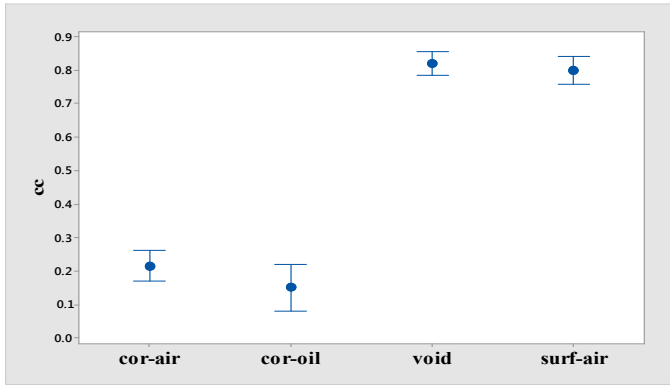


Fig. 4: Comparison of cc for different PD sources.

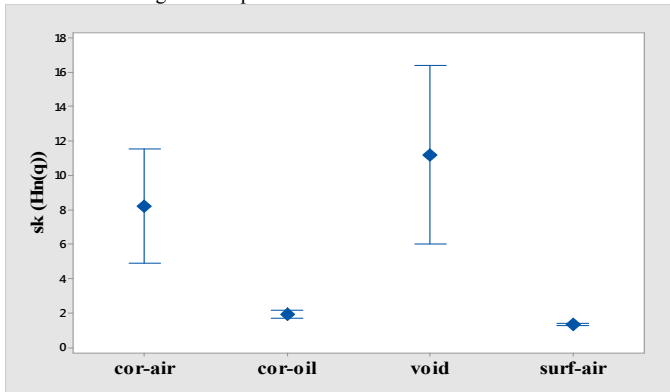


Fig. 5: Comparison of $sk(H_n(q)+)$ for different PD sources.

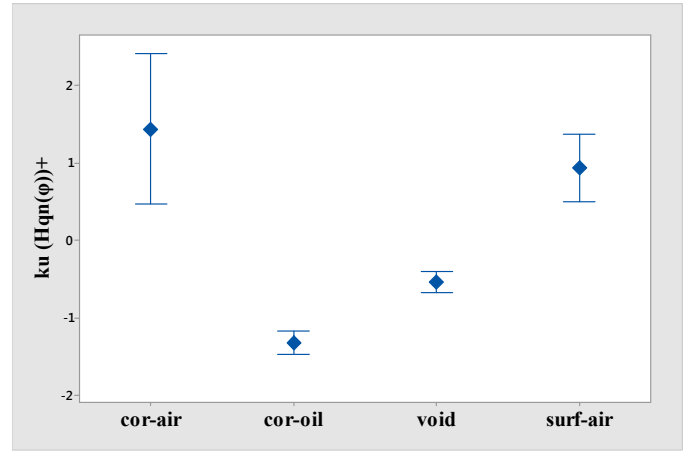


Fig. 6: Comparison of $ku(H_{qn}(\varphi)+)$ for different PD sources.

VI. SIMULATION RESULTS

In this section, emphasis would be drawn to the behavior of ANN and MLR in classifying and discriminating PD patterns of corona in air, corona in oil, internal PDs in voids and surface PDs. The training and testing parameters for ANN and MLR consist of statistical parameters obtained from the $H_{qn}(\varphi)$, $H_n(q)$ and $H_n(\varphi)$ distributions in both the positive and negative voltage half cycles. Two strategies are employed. Firstly, the ANN is trained with either (corona in air, corona in oil, internal PDs and surface PDs) and then tested with the others. Similar strategy is then applied for the other 3 other PD faults. The input parameters are the sk and ku of the $(H_n(\varphi)+, H_n(\varphi)-, H_{qn}(\varphi)+$ and $H_{qn}(\varphi)-)$, Q , cc and mcc . The output parameters are chosen to be $[0\ 0]$, $[0\ 1]$, $[1\ 0]$ and $[1\ 1]$ for the corona in air, corona in oil, voids, surface discharges classification. For each PD defect, 24 samples are applied as training fingerprints while remaining 8 are the testing parameters.

Due to unstable behavior of the ANN, a number of iterations of the ANN result were obtained with different initial states in order to obtain the overall average performance for a more reliable PD diagnosis. After several trial and errors, 8 hidden layers, momentum rate of 0.4 and learning rate of 0.04 are chosen for the ANN model. On the other hand, the MLR is trained in order to determine the weight matrix β . The input data for each PD faults are normalized in order to reduce the variance.

Table 1 compares the classification results from using ANN and MLR. The results show that ANN and MLR are capable of recognizing the PD faults. However, for ANN or MLR trained and tested with the same PD defects, the ANN appears to demonstrate higher recognition rate. Recognition efficiency of 96% has been obtained when training the ANN with corona in oil and testing with the same corona in oil. However, for the ANN and MLR trained and tested with different PD defects, the

MLR generally appears to be more sensitive in discriminating the defects. Recognition rate of 31% was recorded when training MLR with corona in air and testing carried out with surface PD in air.

Table 1: Comparison of classification results using ANN and MLR.

Training data		Testing data and the corresponding recognition rate			
		cor-air	cor-oil	int-void	surf-air
ANN	cor-air	95%	75%	70%	63%
	cor-oil	74%	96%	72%	73%
	int-void	67%	69%	95%	82%
	surf-air	65%	77%	79%	96%
MLR	cor-air	81%	66%	58%	31%
	cor-oil	62%	83%	69%	41%
	int-void	61%	63%	88%	58%
	surf-air	40%	64%	59%	82%

VII. CONCLUSION AND FUTURE WORK

This paper has compared the capabilities of the ANN and MLR for recognizing PD defects of corona in air, corona in oil, internal PD in voids and surface PDs. Statistical φ - q - n PD fingerprints have been applied for training and testing both the ANN and MLR. The result shows that the ANN is better suited for recognizing the same PD defects but the MLR has shown more sensitivity in discriminating them. The implication of the results is that both ANN and MLR can be utilized simultaneously for both online and offline PD detection but their performance depends on the training and testing parameters used. Future work concentrates on applying denoising techniques for PD evaluation in order to determine the robust pattern recognition tool between ANN and MLR.

ACKNOWLEDGEMENT

This paper is based on work supported by the Ministry of Higher Education (MOHE) of Malaysia under grant

20160104FRGS. Any opinions, findings and conclusion or recommendation expressed in this paper are those of the authors and do not necessarily reflect those of the Ministry of Higher Education (MOHE) of Malaysia.

REFERENCES

- [1] E. Gulski and A. Krivda, "Neural network as a tool for recognition of partial discharges," *IEEE Transaction on Electrical Insulation*, vol.28, no.6 ,pp. 984-1001, 1993.
- [2] A. Krivda, automated recognition of partial discharges, *IEEE Trans on Dielectrics and Electrical Insulation*, vol.2, no.5, 792-821, 1995.
- [3] P. Gill. *Electrical power equipment maintenance and testing*. CRC press, 2008.
- [4] A. Abubakar Mas'ud, B.G.Stewart, S.G.McMeekin, Application of Ensemble neural networks for classifying partial discharge patterns, *Electric Power System Research* 110 , 154-162, 2014.
- [5] S, Ludpa., S.,N,Pattanadech,M,Leelajindakrairerk. Pattern classification of partial discharges in high voltage equipment by the regression analysis In;Proceedings of ECTI-CON, pp921-924, 2008.
- [6] IEC 60270 , British standard guide for partial discharge measurement, 2001.
- [7] N. Giaot Rinh, Partial discharge XIX: Discharge in air part I: Physical mechanisms. *Electrical Insulation Magazine*, IEEE 11, no. 2, 23-29 , 1995.
- [8] Niasar, M. Ghaffarian, et al. Partial discharge characteristics due to air and water vapor bubbles in oil. *International Symposium on High Voltage Engineering*, 2011.
- [9] P. Cunningham, J. Cama and S. Jacob, Stability Problems with the Artificial Neural Networks and the Ensemble Solution, *Art Intelligence in Medicine*, vol.20, no.3, 217-225, 2000.
- [10] S. Haykin, *Neural networks: A comprehensive foundation*, Prentice Hall, 1998.
- [11] Ngo, Theresa Hoang Diem, and C. A. La Puente. The steps to follow in a multiple regression analysis. *Proceedings of the SAS Global Forum 2012 Conference*, Orlando, Florida, April 22–25, 2012.
- [12] A. Mas'ud, R. Albarracín, J. Ardila-Rey, F. Muhammad-Sukki, H. Illias, N. Bani, and A. Munir, "Artificial Neural Network Application for Partial Discharge Recognition: Survey and Future Directions," *Energies*, vol. 9, no. 8, p. 574, Jul. 2016.